The Canadian Mineralogist
Vol. 40, pp. 711-723 (2002)

HONGSHIITE, PtCu, FROM ITABIRITE-HOSTED Au–Pd–Pt MINERALIZATION (JACUTINGA), ITABIRA DISTRICT, MINAS GERAIS, BRAZIL

ROGERIO KWITKO§

Centro de Desenvolvimento Mineral, Companhia Vale do Rio Doce, BR 262/ km 296, 33030-970 Santa Luzia – MG, Brazil

ALEXANDRE R. CABRAL§ AND BERND LEHMANN

Institut für Mineralogie und Mineralische Rohstoffe, Technische Universität Clausthal, Adolph-Roemer-Str. 2A, D-38678 Clausthal-Zellerfeld, Germany

J.H.GILLES LAFLAMME and LOUIS J. CABRI

Canada Centre for Mineral and Energy Technology, 555 Booth Street, Ottawa, Ontario K1A 0G1, Canada

ALAN J. CRIDDLE

Mineral Science and Systematics Division, Department of Mineralogy, The Natural History Museum, London SW7 5BD, U.K.

HENRY F. GALBIATTI

Diretoria de Ferrosos Sul, Companhia Vale do Rio Doce, 35900-900 Itabira-MG, Brazil

ABSTRACT

Hongshiite occurs associated with palladian gold, and more rarely with native platinum, in the sulfide-free, hematite-rich jacutinga mineralization of the Quadrilátero Ferrífero, central Minas Gerais, Brazil. Hongshiite occurs in grains up to about 1.5 mm in cross-section. The crystals (>0.1 mm) are generally covered by a porous rim from which copper is preferentially leached, eventually forming a rind of nearly pure native platinum. The morphological and chemical features of hongshiite are similar to features caused by the weathering of primary gold in a lateritic environment. Submicrometer-sized crystals, acicular in shape, replace an octahedral precursor phase, interpreted to be magnetite. The magnetite could have acted as a local redox barrier to the passage of oxidizing hydrothermal fluids leading to hongshiite precipitation. Sperrylite, isomertieite, atheneite, sudovikovite, a "guanglinite"-like phase, an undefined copper selenide, and barite occur as euhedral to anhedral inclusions in the larger crystals of hongshiite. Patches of a Au–Cu–Pt alloy within hongshiite have a composition nearly intermediate between tetra-auricupride and hongshiite, and could be called platinian tetra-auricupride, suggesting an extension of a solid solution toward hongshiite. The presence of tiny rosette-like crystals of native palladium in the auriferous jacutinga mineralization is also documented.

Keywords: hongshiite, sudovikovite, platinum-group minerals, palladium rosettes, Au–Pd–Pt jacutinga mineralization, Itabira Iron Formation, Quadrilátero Ferrífero, Minas Gerais, Brazil.

SOMMAIRE

La hongshiite se trouve associée à l'or palladifère, et plus rarement avec le platine natif, dans une zone minéralisée de type jacutinga dépourvue de sulfure et enrichie en hématite dans le "Quadrilátero Ferrífero", Minas Gerais central, au Brésil. Elle se présente en grains atteignant jusqu'à environ 1.5 mm de diamètre. En général, les cristaux (>0.1 mm) sont recouverts d'une gaine poreuse de laquelle le cuivre a été lessivé, menant à une bordure faite de platine presque pur. Le développement morphologique et chimique de cette bordure ressemble donc à celle des grains d'or primaire lessivés dans un milieu latéritique. Des cristaux aciculaires submicrométriques ont remplacé un précurseur octaédrique, probablement la magnétite, qui aurait ralenti localement l'oxydation due à la phase fluide hydrothermale, menant à la précipitation de la hongshiite. Sperrylite, isomertieïte, athénéite, sudovikovite, une phase de type "guanglinite", un séléniure de cuivre non défini, et la barite sont incluses dans les plus gros cristaux de hongshiite. Des domaines d'un alliage Au–Cu–Pt dans la hongshiite possèdent une composition presque intermédiaire

§ *E-mail addresses*: kwitko@cvrd.com.br, cabral@min.tu-clausthal.de

entre la tétra-auricupride et la hongshiite, et donc de tétra-auricupride platinifère, serait une indication d'une extension de la solution solide vers la hongshiite. Nous documentons aussi la présence de très petits cristaux de palladium en rosettes dans le minerai aurifère de type jacutinga.

(Traduit par la Rédaction)

Mots-clés: hongshiite, sudovikovite, minéraux du groupe du platine, rosettes de palladium, minéralisation Au–Pd–Pt de type jacutinga, Formation de fer Itabira, Quadrilátero Ferrífero, Minas Gerais, Brésil.

Introduction

The characterization of the mineral hongshiite has had a complicated history. Hongshiite was originally described as hexagonal PtCuAs (without IMA–CNMMN approval) from Pt-bearing mafic and ultramafic intrusions in the Yen (?), Yanshan and Tibet regions, China, by Yu *et al*. (1974); these same authors are reported to have later redetermined the composition to be PtCu (Peng *et al*. 1978). A review of the first article is given by Chao & Cabri (1976), and of the latter article by Cabri (1980). Ding (1980) stated that hongshiite is rhombohedral PtCu (*a* 10.71, *c* 13.20 Å), as is "isoplatinocopper", formerly considered to be cubic PtCu (Cabri & Chao 1978), and that hongshiite (as redefined) has precedence over "isoplatinocopper". In later publications, Yu (1982, 1986) confirmed the composition as PtCu, reported a unit cell of *a* 10.713, *c* 13.192 Å, with three possible rhombohedral space-groups. Yu's data were re-indexed, and a new unit cell was calculated in PDF 42–1326, *a* 10.703, *c* 13.197 Å, space group *R*3*m*. [Note added at the proof stage: Yu (2001) provided new electron-microprobe and powder-diffraction data for hongshiite.]

Though hongshiite is a rare platinum-group mineral (PGM), it has been reported from several deposits outside China, in association with Pt–Fe and Os–Ir–Ru alloys (Cabri & Laflamme 1997, Okrugin *et al*. 1999, Tolstykh *et al*. 1996, 1997, 2000, Weiser & Schmidt-Thomé 1993), as well as with palladian and Pt–Cu-bearing gold (Törnroos & Vuorelainen 1987). Apparently, no occurrences have ever been reported from rocks other than mafic-ultramafic and associated placer deposits.

In this contribution, we document the unusual occurrence of hongshiite in hematite-rich, auriferous veins hosted by itabirite of the Paleoproterozoic Itabira Iron Formation at the Cauê and Conceição iron ore mines. A number of platinum-group minerals found as inclusions in hongshiite also are described, including the second occurrence of sudovikovite (Polekhovskii *et al*. 1997). Although bearing no direct relation to hongshiite, a record of delicate rosette-like crystals of palladium from the same assemblage is given.

Geological Setting

The world-class Itabira iron-ore district is part of the Quadrilátero Ferrífero of Minas Gerais, Brazil. The iron ore deposits are hosted by the Itabira Iron Formation of Harder & Chamberlin (1915), *i.e.*, the Itabira Group of Dorr (1969). The Itabira Group is the middle unit of the Paleoproterozoic Minas Supergroup, which consists of a thick continuous sequence of chemical sediments divided into (i) the Cauê Formation, a lower unit of oxide-facies iron formation, and (ii) the Gandarela Formation, an upper sequence of dolomitic itabirite and dolomite. Below the Itabira Group lies the Caraça Group, which is composed of quartzite, conglomerate, micaceous schist and phyllite. The predominantly clastic sediments of the Piracicaba Group unconformably overlie the Itabira Group. The Minas Supergroup rests upon the Archean volcano-sedimentary Rio das Velhas Supergroup. These metasedimentary units form belts that surround Archaean basement domes, defining a dome-and-keel structure. Two tectonic events affected the Quadrilátero Ferrífero: the Transamazonian Orogeny (2.1–2.0 Ga) and the Pan-African – Brasiliano Orogeny (0.8–0.6 Ga). The latter produced pervasive tectonic fabrics (mylonitic foliation, crenulation cleavage, stretching lineation) (Chemale 1987, Chemale *et al.* 1994, Alkmim & Marshak 1998, Hippertt & Davis 2000). Compilations of the geology of the Quadrilátero Ferrífero can be found in Klein & Ladeira (2000) and Lobato *et al.* (2001).

The geological context of the Itabira district was summarized by Dorr & Barbosa (1963), who characterized three synclines (Cauê, Conceição and Dois Córregos) and their connecting anticlines (Chacrinha and Periquito), as subsidiary folds of a major syncline. The metamorphic conditions at Itabira were more extreme than those in the western and central parts of the Quadrilátero Ferrífero. Oxygen isotope data suggest metamorphic temperatures up to 660°C (Hoefs *et al.* 1982). It has been assumed that itabirites have been weathered since Cretaceous times (Dorr & Barbosa 1963).

Jacutinga: Auriferous Hydrothermal Mineralization in Itabirite

Gold hosted by itabirite and hematite iron ore in the Quadrilátero Ferrífero has been mined since the 18th century. In fact, Itabira began as a gold-mining center after the first discoveries were made in 1720. Known regionally as jacutinga, the vein-style gold mineralization is characteristically sulfide-free and consists pre-

dominantly of soft hematite with subordinate kaolinite, talc, manganese oxide and goethite (Hussak 1906). Quartz typically occurs in centimetric clusters with specular hematite. Gold is alloyed with palladium (Hussak 1906), a diagnostic element in the jacutinga deposits of the Quadrilátero Ferrífero. In particular, a number of palladium minerals were discovered or redefined from Itabira, such as arsenopalladinite and atheneite (Clark *et al.* 1974, Cabri *et al.* 1975, 1977), palladinite (Jedwab *et al.* 1993), and palladseite (Davis *et al.* 1977). Recent studies on the Pd mineralogy of Itabira were carried out by Olivo and coworkers (Olivo *et al.* 1995, 2001, Olivo & Gauthier 1995, Olivo & Gammons 1996).

The astonishingly high grades, reaching a few kilograms of gold per tonne, motivated early attempts to understand the genesis of the jacutinga ore [Cabral *et al.* (2001) for references]. The jacutinga mineralization occurs as a few decimeter-wide veins that cross-cut the friable itabirite. The host itabirite is complexly folded and has a pervasive mylonitic foliation (S1). Two contrasting concepts have been advanced regarding the jacutinga mineralization. The origin of the Au–Pd mineralization may have been synchronous with ductile D1 shearing at peak conditions of metamorphism (approximately 600°C), assuming that the orebodies are parallel to the S1 mylonitic foliation or to the stretching lineation (Olivo *et al.* 1995). Lead isotopic data for palladian gold, quartz and hematite yielded an errorchron age of 1.83 ± 0.10 Ga (mean squared weighted deviation of 7.55), which would correspond to the late Transamazonian Orogeny (Olivo *et al.* 1996). The other view, based on the mapping of working faces by mine geologists, indicates that the auriferous orebodies are controlled by a set of fractures, which truncate the S1 foliation (Galbiatti 1999). This brittle–ductile event is tentatively correlated with the Pan-African – Brasiliano Orogeny (Guimarães 1970, Galbiatti 1999, Varajão *et al.* 2000)

Methodology

Heavy-mineral concentrates were obtained by panning of the jacutinga ore from the Central and Conceição orebodies at the Cauê and Conceição mines, respectively. Selected grains were mounted on conductive holders for mineral search, identification and imaging with a Philips XL30 SEM at the Companhia Vale do Rio Doce (CVRD), Brazil. The system is equipped with an EDAX iDX4 Si(Li) super-ultrathin-window energy-dispersion spectrometer (EDS) as a detector, and the ED spectra were acquired under acceleration voltage of 20 kV.

Some grains were also mounted in resin to prepare polished sections for ore microscopy and electron-microprobe analysis using a Cameca SX 100 at the Technische Universität Clausthal under operating conditions of 20 kV and 40 nA. The standards used were pure metals for Au, Pt, Pd, Rh and Se, all with the $L\alpha$ emission line, and Cu with the $K\alpha$ line. Other elements sought were (standards in parentheses): Hg$L\alpha$ (HgTe), Sn$L\alpha$ (SnO_2), Sb$L\beta$ (InSb), As$L\beta$ (GaAs) and S$K\alpha$ (PbS).

An additional electron-microprobe investigation was carried out at CANMET using a JEOL 733 electron microprobe, operated at 20 kV with a beam current (cup reading) of 20 nA. The following X-ray emission lines (and standards) were used: Pt$L\alpha$, Cu$K\alpha$ (PtCu), Fe$K\alpha$ (Pt_3Fe), As$L\alpha$ (InAs), Pd$L\alpha$, Os$M\alpha$, Ir$L\alpha$, Ru$L\alpha$, Rh$L\alpha$, Ni$K\alpha$, Sb$L\alpha$, Se$L\alpha$ and Au$L\alpha$ (metals). Counting time was of the order of 10–40 s, and raw data were corrected using a ZAF program. Additional corrections were made to correct for the enhancement of Rh$L\alpha$ by PtM_2N_4.

X-ray-diffraction analysis at CANMET was done with a 114.6 mm Gandolfi camera using Co radiation (Co$K\alpha$ = 1.79021 Å) and a Fe filter. The film measurements were corrected for shrinkage, but no internal standard was used.

The reflectance data were measured at the Natural History Museum with a Zeiss microscope spectrophotometer (MPM 800) relative to a WTiC reflectance standard (314). Measurements in immersion oil were made with Zeiss oil N_D = 1.515. The data were collected at intervals of 10 nm from 400 to 700 nm, the aperture of the grating monochromator being set at 5 nm. Objectives of ×50 were used, and the diameter of the measured fields was set at a constant 5 μm.

Hongshiite from Itabira

Hongshiite occurs as: (i) crystals of irregular shape up to 1.5 mm across (Fig. 1a), in some cases showing a conchoidal (?) type of fracture (Fig. 1b), and attached to palladian gold (Fig. 1c), (ii) as anhedral grains with a pitted surface showing dissolution pits (Fig. 1d), (iii) as grains partially replaced by a Pt–Cu phase with a porous texture (Figs. 1e, f), (iv) as fine-grained aggregates with native platinum (Fig. 1g), (iv) as aggregates showing stepped facets (Fig. 1h), and (v) as fine-grained aggregates associated with palladian gold (Fig. 2a). A closer investigation of the latter reveals that the aggregate is composed of euhedral octahedral crystals (Fig. 2b) replaced by slender crystals of hongshiite <1 μm across (Fig. 2c).

Electron-microprobe analyses of Pt–Cu grains (Table 1) indicate that their Pt:Cu atomic ratios correspond to that of hongshiite, with traces of Au and Pd, up to 0.82 and 0.30 wt.%, respectively. As the PtM_2N_4 X-ray emission line interferes with Rh$L\alpha$, 1 wt.% Pt accounts for 0.0042 wt.% Rh false concentration (Cabri & Laflamme 1981, Nixon *et al.* 1990). In the case of hongshiite, with about 75 wt.% Pt, this interference might not only explain the average of 0.3 wt.% Rh obtained during preliminary analyses, but also the Rh content (0.29–0.39 wt.%) reported by Okrugin *et al.* (1999).

Analysis of the porous rim found on some hongshiite crystals (Figs. 1e, f) shows depletion in copper and rela-

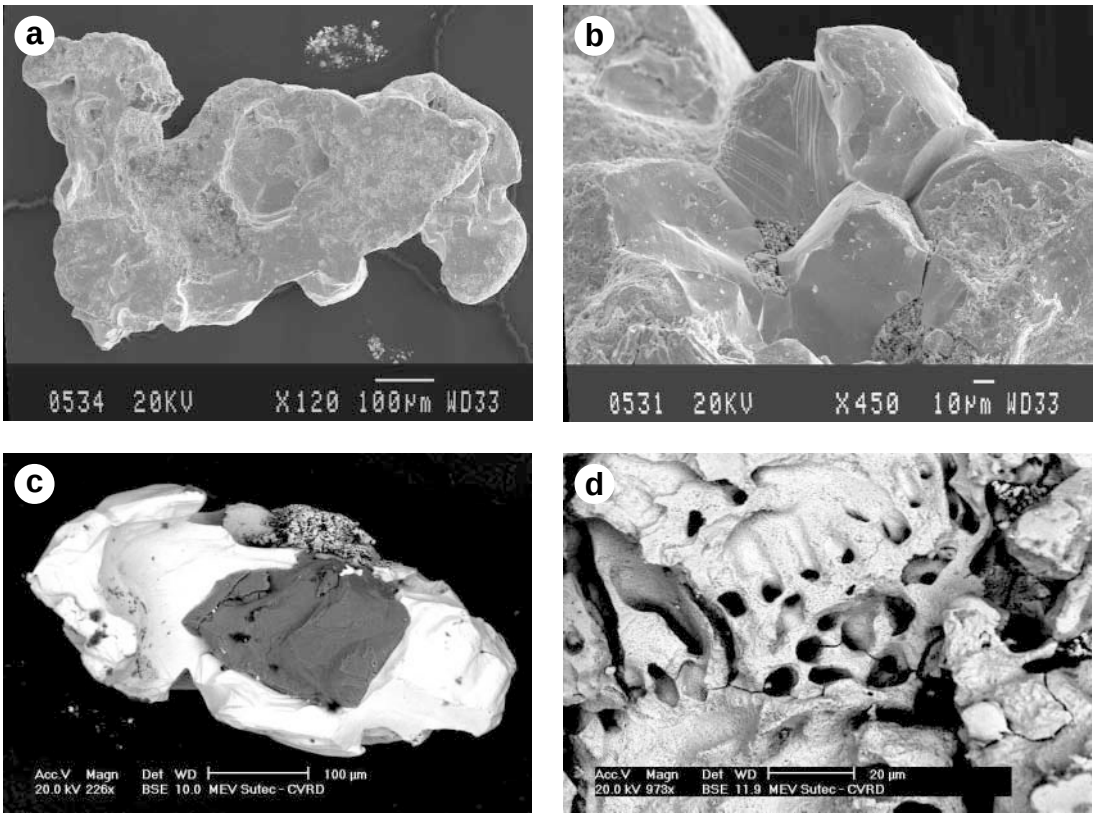

TABLE 1. COMPOSITION OF HONGSHIITE FROM THE ITABIRA DISTRICT

	1	2	3	4	5	6	7	8	9*	10	11	12	13**
Pt wt.%	73.66	74.81	75.02	74.85	74.38	74.69	74.77	75.51	75.49	75.81	75.54	75.53	75.00
Cu	24.28	23.73	24.23	23.82	24.10	24.05	23.99	24.13	24.55	24.35	24.20	24.30	24.35
Au	0.57	n.d.	0.43	0.82	0.27	n.d.	n.d.	n.d.	0.24	0.13	0.12	0.72	0.33
Pd	0.20	0.24	0.06	0.12	0.20	0.11	0.24	0.30	0.10	0.17	0.19	0.12	0.16
Total	98.71	98.78	99.74	99.61	98.95	98.85	99.00	99.94	100.38	100.46	100.05	100.67	99.84
Formula based on two atoms per formula unit (*apfu*)													
Pt *apfu*	0.988	1.010	1.001	1.005	0.998	1.004	1.004	1.006	0.998	1.004	1.005	1.000	0.998
Cu	1.000	0.984	0.992	0.982	0.993	0.993	0.990	0.987	0.996	0.990	0.989	0.988	0.994
Au	0.008	–	0.006	0.011	0.004	–	–	–	0.003	0.002	0.002	0.009	0.004
Pd	0.005	0.006	0.001	0.003	0.005	0.003	0.006	0.007	0.002	0.004	0.005	0.003	0.004

The electron-microprobe analyses 1–8 were done at the Technische Universität Clausthal; n.d. = not detected. Analyses 9–13 were done at CANMET; Os, Ir, Ru, Rh, Fe, Ni, Sb and As were sought, but were not detected with minimum detection limits (MDL) of 0.18, 0.10, 0.06, 0.07, 0.02, 0.02, 0.05 and 0.04 wt.% respectively. * Grain with platinian tetra-auricupride, also used for reflectance measurements. ** Grain studied by X-ray diffraction.

tive enrichment in platinum (Table 2, Fig. 3). Unfortunately, it was not possible to make a series of analyses across a single porous leached rim because of a poor polished surface and the porosity. Thus, the results shown in Table 2 and Figure 3 were acquired from three different grains.

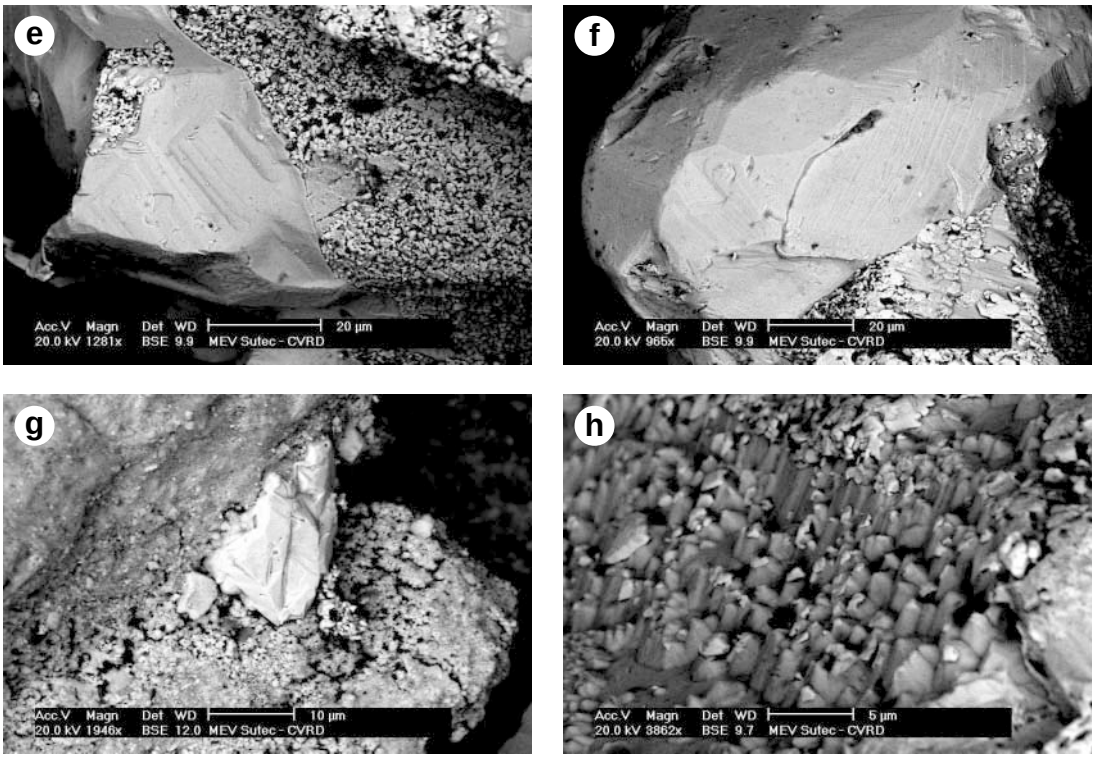

FIG. 1. Textural aspects of hongshiite and associated minerals from the Cauê iron-ore mine. a. Secondary electron image (SEI) of hongshiite grains showing their irregular shape, rounded corners, and cavities. b. SEI showing the possible conchoidal fracture. c. Back-scattered electron image (BSE) of hongshiite from the Central orebody; gold particle (white) associated with quartz (dark, center) and hongshiite (gray, upper part) with porous texture. d. BSE image of the pitted "porous" surface of a hongshiite grain (Central orebody). e. BSE image of a hongshiite crystal (Central orebody), partially rimmed by a porous Pt-rich, Cu-poor phase. f. The same crystal as shown in e, with details of the crystal faces. g. BSE image of native platinum (white, center) associated with fine-grained hongshiite (Central orebody). h. BSE image of hongshiite showing stepped facets (Central orebody).

TABLE 2. COMPOSITION* OF POROUS RIM ON HONGSHIITE, ITABIRA DISTRICT

	1	2	3	4	5	6	7
Pt wt.%	89.60	90.19	90.79	91.03	91.80	100.44	90.61
Cu	6.20	2.05	8.01	6.36	6.23	0.49	1.23
Au	1.34	3.65	0.75	1.03	0.85	n.d.	2.99
Pd	0.83	0.97	0.35	0.32	0.33	0.28	1.33
Total	97.97	96.86	99.90	98.74	99.21	101.21	96.16
Pt at.%	80.36	88.53	77.75	81.16	81.69	98.03	90.80
Cu	17.09	6.18	21.06	17.41	17.02	1.47	3.79
Au	1.19	3.55	0.64	0.91	0.75	–	2.97
Pd	1.36	1.75	0.55	0.52	0.54	0.50	2.44

* Electron-microprobe data; n.d.: not detected.

Irregular areas of a Au–Cu–Pt alloy occur as patches within hongshiite. The Au–Cu–Pt alloy consists of about 45.5 wt.% Au, 27.5 wt.% Pt and 25.0 wt.% Cu, with subordinate amounts of Pd and As (Table 3, Figs. 4, 5). A comparison with the literature shows that the alloy has the highest known Pt content, about 18 at.% Pt, and has a composition in between hongshiite and tetra-auricupride (Fig. 6). This phase corresponds to $(Au_{0.58}Pt_{0.36}Pd_{0.06}As_{0.01})_{\Sigma 1.01}Cu_{0.99}$, and could be called platinian tetra-auricupride. Because the symmetry of tetra-auricupride (tetragonal) differs from the rhombohedral symmetry of hongshiite, we assume that this phase represents the most Pt-rich occurrence to date.

In plane-polarized light, the hongshiite and the irregularly shaped inclusions of platinian tetra-auricupride are best distinguished at low magnification (this is because of the difference in their polishing hardness), though neither mineral is perceptibly bireflectant or pleochroic. Between crossed polars, both minerals are

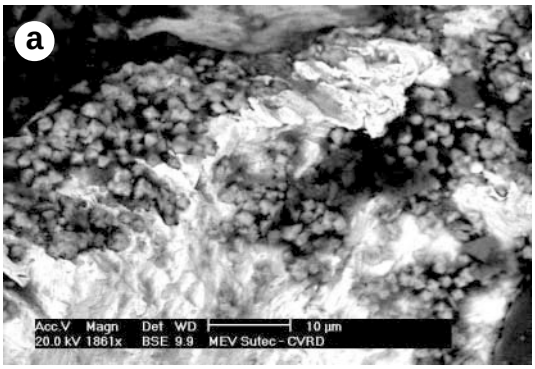

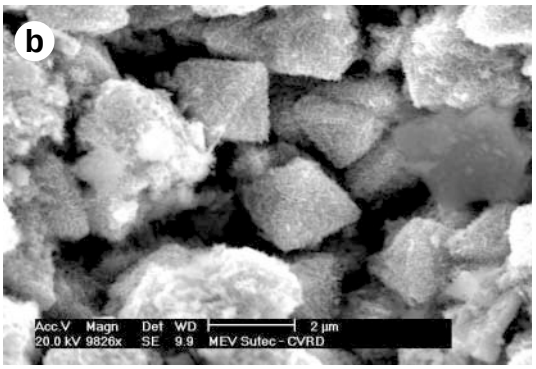

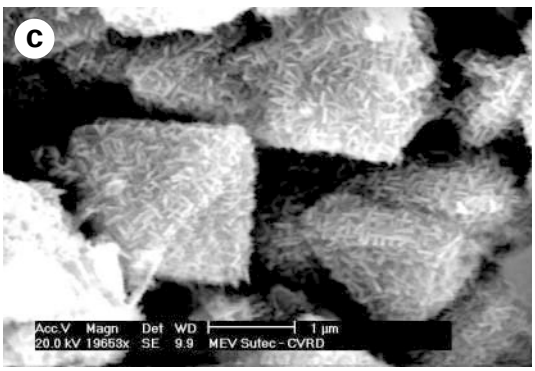

FIG. 2. BSE images of hongshiite from the Conceição iron-ore mine (Conceição orebody). a. Native gold (white) partially overgrown by fine-grained crystals of hongshiite (gray). b. Higher-magnification view, showing the octahedra. c. A detailed view of the previous image shows that hongshiite occurs as a mesh of thin elongate crystals, suggesting pseudomorphism after a cubic phase.

TABLE 3. COMPOSITION* OF Au–Cu–Pt ALLOY, ITABIRA DISTRICT

	1	2	3		1	2	3
Au wt.%	45.48	44.96	45.90	Au *apfu*	0.582	0.578	0.587
Pt	27.44	27.53	27.47	Pt	0.355	0.357	0.355
Pd	2.43	2.53	2.37	Pd	0.058	0.060	0.056
As	0.38	0.40	0.33	As	0.013	0.014	0.011
Cu	25.00	24.89	25.02				
				Sum	1.008	1.009	1.009
total	100.73	100.31	101.09	Cu	0.992	0.991	0.991

There are two atoms per formula unit (*apfu*).

moderately anisotropic; the rotation tints of hongshiite vary from a coppery brown to a bright blue, whereas those of the slightly more anisotropic platinian tetra-auricupride are a bright, lightly pinkish buff color at 45° from extinction.

The reflectance spectra (Fig. 7) confirm what the microscopist sees, *i.e.*, the two quite different species reflect light almost identically within the visible spectrum. Perhaps the only distinction, a slight difference in the slope of the dispersion, is revealed in the color values in Table 4, where the excitation purity (P_e%) or saturation of the hue of the platinian tetra-auricupride is greater than that of hongshiite. The data presented on

TABLE 4. REFLECTANCE DATA (%) AND COLOR VALUES FOR HONGSHIITE AND PLATINIAN TETRA-AURICUPRIDE

	Hongshiite				Tetra-auricupride			
λ nm	R_1	R_2	$^{inn}R_1$	$^{inn}R_2$	R_1	R_2	$^{inn}R_1$	$^{inn}R_2$
400	51.6	52.85	40.35	41.5	49.4	50.7	38.4	39.5
420	53.15	54.6	41.85	42.9	51.2	52.5	40.2	41.3
440	54.7	56.1	43.2	44.3	52.9	54.3	41.75	42.85
460	55.9	57.25	44.25	45.2	54.45	55.7	43.1	44.1
480	57.2	58.6	45.25	46.1	55.7	57.15	44.35	45.5
500	58.1	59.55	46.15	46.95	57.05	58.5	45.45	46.65
520	59.0	60.5	46.95	47.7	58.1	59.55	46.65	47.9
540	59.85	61.25	47.8	48.5	59.0	60.4	47.45	48.8
560	60.4	62.05	48.5	49.2	60.0	61.35	48.5	49.85
580	61.05	62.7	49.1	49.8	60.75	62.2	49.5	51.0
600	61.85	63.5	50.0	50.5	61.55	63.1	50.5	51.95
620	62.35	64.1	50.65	51.1	62.6	63.8	51.5	52.7
640	63.0	64.8	51.35	51.85	63.4	64.6	52.0	53.0
660	63.6	65.3	51.8	52.3	64.25	65.0	52.8	53.55
680	64.15	66.1	52.5	52.9	65.1	65.6	54.1	54.5
700	64.7	66.6	52.9	53.35	66.75	67.0	55.4	55.55
	COM minimum wavelengths							
470	56.55	57.9	44.75	45.65	55.05	56.45	43.75	44.8
546	60.0	61.5	48.0	48.7	59.3	60.7	47.75	49.15
589	61.4	63.1	49.55	50.15	61.15	62.65	50.0	51.5
650	63.3	65.05	51.6	52.1	63.85	64.8	52.4	53.3
	Color values: A Illuminant (~2856 K)							
x	0.456	0.456	0.458	0.457	0.458	0.458	0.461	0.461
y	0.410	0.410	0.410	0.410	0.411	0.411	0.411	0.411
Y%	60.8	62.4	48.9	49.5	60.4	61.8	49.1	50.4
λ_d	587	587	588	588	587	587	588	587
P_e%	7.5	7.7	8.9	8.2	9.5	9.2	11.6	11.8
	Color values: C Illuminant (~6774 K)							
x	0.320	0.320	0.322	0.321	0.322	0.322	0.326	0.325
y	0.326	0.326	0.328	0.327	0.328	0.328	0.331	0.331
Y%	60.3	61.8	48.3	49.0	59.7	61.1	48.3	49.7
λ_d	577	577	578	578	578	577	579	578
P_e%	5.3	5.3	6.2	5.7	6.5	6.4	8.0	8.1

hongshiite show higher values of reflectance, measured in air, than those reported by Okrugin *et al.* (1999), which range from (50.0, 50.7) at 420 nm to (60.7, 62.2) at 700 nm for R_1, R_2.

Two grains of hongshiite examined by X-ray diffraction were found to contain extra reflections at 6.057 and 2.141 Å, with respect to pattern 42–1326 from ICDD. These additional reflections could not be indexed on the rhombohedral cell of Ding (1980), and we were unable to obtain unequivocal indices because of the lack of single-crystal information. X-ray powder-diffraction data for one grain (Table 1, anal. 13) are given in Table 5, and compared to those of Ding (1980).

Other Related Minerals

A number of euhedral to anhedral inclusions ranging from 5 to 25 μm were found in hongshiite. Although their microprobe-established compositions probably reflect some Pt and Cu from the hongshiite matrix (Table 6), the stoichiometry indicates that these minerals are atheneite, $(Pd,Hg)_3As$, isomertieite, $Pd_{11}(Sb_2As_2)$, sperrylite, $PtAs_2$, and sudovikovite, $PtSe_2$. This is the second occurrence of sudovikovite, shown in Figure 8. The sudovikovite was originally reported to occur in a roscoelite – chromian phengite – dolomite veinlet 7–10 cm thick, formed as a result of hydrother-

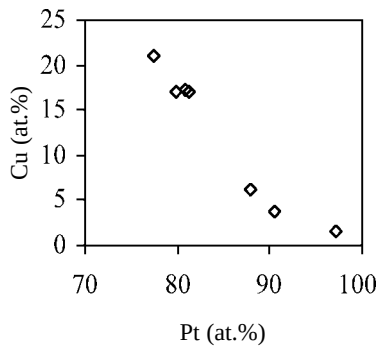

FIG. 3. Variation diagram showing Cu *versus* Pt contents from the porous rim on hongshiite crystals (see text). The electron-microprobe data are given in Table 2.

TABLE 5. X-RAY-DIFFRACTION DATA FOR HONGSHIITE, ITABIRA DISTRICT

I est.*	*d* meas.*	*hkl**	*I* est.**	*d* meas.**	*hkl***
10	6.057				
30	4.278	021, 003	30	4.35	003
			<10	3.39	113
			20	3.05	300
20	2.299	205, 223, 401	10	2.295	205
100	2.194	006, 042	100	2.199	006
30	2.141				
90	1.888	404	80	1.895	404
10	1.728	241, 045, 027	<10	1.738	241
			10	1.489	416
5	1.444	603, 063, 425, 407, 009	10	1.450	603
50	1.349	048, 440	50	1.350	048
50	1.325	309, 039, 048	50	1.325	309

* Composition 13 in Table 1. ** Ding (1980).

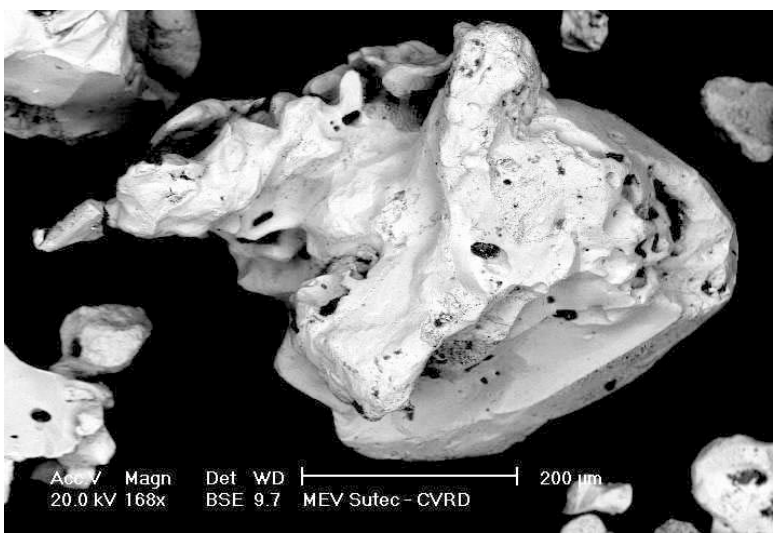

FIG. 4. BSE image of an alloy with a composition intermediate between hongshiite and tetra-auricupride (Central orebody).

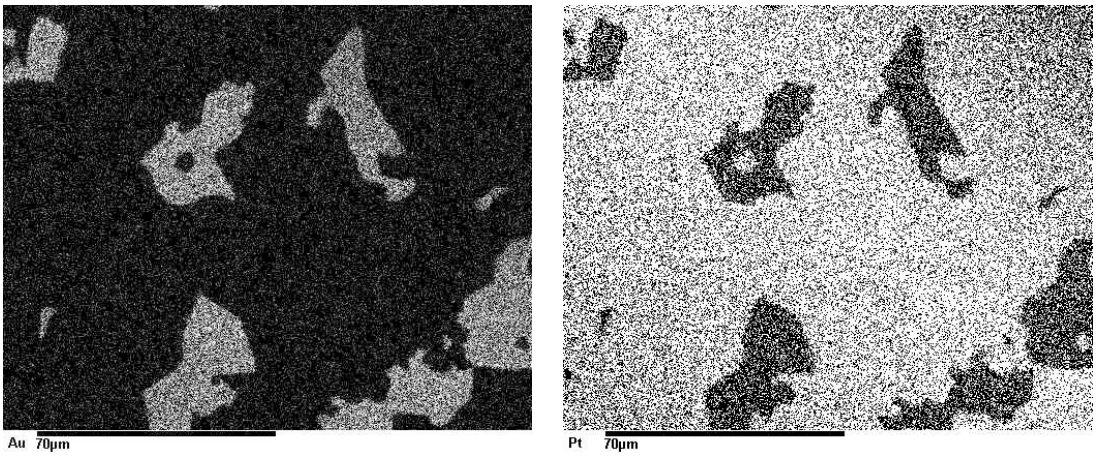

FIG. 5. X-ray element-distribution maps of hongshiite. a. Au*L*α of hongshiite grain (Table 1, anal. 9), indicating the irregular patches of Au–Cu–Pt alloy. b. Pt*L*α of same area in the hongshiite grain, showing the lesser Pt content of the irregular patches of Au–Cu–Pt alloy.

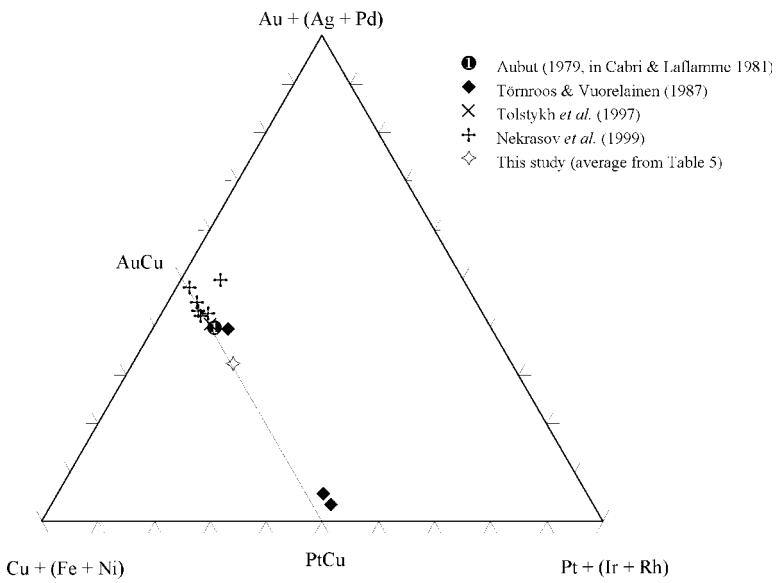

FIG. 6. Compositions of Au–Cu–Pt alloys plotted on along the join tetra-auricupride (AuCu) – hongshiite (PtCu).

mal metasomatic activity, at the Padma uranium–vanadium deposit on the Zaonega Peninsula, Russia (Polekhovskii *et al.* 1997). There, it was found as irregular 10 to 180 μm grains in clausthalite. Table 6 also includes data on a mineral similar to "guanglinite", $Pd_3(As,Sb)$ (Cabri 1980, Peng *et al.* 1978), which has never been submitted for approval to the IMA–CNMMN. In addition, an undefined copper selenide (maximum size of 30 μm) was also found in three of the grains of Pt–Cu alloy (Fig. 8). Among the minerals found, other than the PGM, are euhedral inclusions (up to 5 μm) of barite and a Mg silicate.

TABLE 6. COMPOSITION OF INCLUSIONS IN HONGSHIITE, ITABIRA DISTRICT

	1	2	3	4	5	6
Pt wt.%	56.46	2.81	1.98	55.78	56.24	1.84
Cu	0.33	1.86	0.84	0.66	1.05	1.26
Pd	n.d.	74.86	67.11	n.d.	n.d.	79.34
Hg	n.a.	n.a.	15.99	n.a.	n.a.	n.a.
Sn	n.d.	0.06	n.d.	n.d.	n.d.	n.d.
As	42.31	8.93	15.86	0.21	0.21	16.93
Sb	n.d.	13.40	n.d.	n.d.	n.d.	3.62
Se	0.46	n.d.	n.d.	42.98	42.87	n.d.
Total	99.56	101.92*	101.78*	99.63	100.37	102.99*
Pt *apfu*	1.002	0.215	0.042	1.019	1.017	0.035
Cu	0.017	0.446	0.055	0.037	0.058	0.078
Pd	–	10.804	2.668	–	–	2.894
Hg	–	–	0.338	–	–	–
Sn	–	0.015	–	–	–	–
Sum	1.019	11.480	3.103	1.056	1.075	3.007
As	1.959	1.829	0.896	0.010	0.010	0.877
Sb	–	1.691	–	–	–	0.116
Se	0.021	–	–	1.934	1.915	–
Sum	1.980	3.520	0.896	1.944	1.925	0.993
Σ *apfu*	3	15	4	3	3	4

* Probable contamination from the surrounding hongshiite matrix. n.d.: not detected, n.a.: not sought. Columns: 1: sperrylite, 2: isomertieite, 3: atheneite, 4–5: sudovikovite, 6: guanglinite-like phase. Electron-microprobe data.

During the investigation of heavy-mineral concentrates from the Aba Leste Inferior jacutinga orebody, Cauê mine, aggregates of native palladium were observed to grow over a mass of iron oxyhydroxide, associated with palladian gold (Fig. 9a). They consist of tiny crystals, whose pattern is formed roughly by the intersection of discs in three orthogonal directions (Figs. 9b, c and d). These rosette-like crystals of palladium are an unusual feature of the assemblage; even though palladium is not directly related to hongshiite, there is inherent interest in this poorly documented species from the Itabira district.

Discussion and Conclusions

The association of hongshiite with palladian gold (Fig. 1c) suggests contemporaneity with gold deposition, but hongshiite appeared relatively late owing to its apparent absence as inclusions in the gold. The preferential leaching of Cu, residual enrichment in Pt (Figs. 1e, f) and the development of dissolution pits on the surface of some hongshiite grains (Fig. 1d) may be a result of weathering under lateritic conditions, similarly to the weathering that affects primary gold (*e.g.*, Colin *et al.* 1997, Varajão *et al.* 2000). However, the associated palladian gold remained unaltered by this process, implying that hongshiite is more susceptible to weathering than palladian gold (*cf.* Varajão *et al.* 2000).

It is interesting to compare the composition of the native platinum (Table 2, anal. 6), *i.e.*, free of base metals (the Cu is likely due to the surrounding hongshiite), which comes from a pitted rim on hongshiite. Its composition is closer to that typically found in hydrothermally precipitated platinum (McDonald *et al.* 1999). This is in contrast to the Pt–Fe alloys associated with ultramafic intrusions (Sweeny 1989, Cabri *et al.* 1996) and stratiform PGE deposits (reviewed in Cabri 1981). Nevertheless, the porous rims are interpreted to be supergene in origin. If confirmed, then it may be assumed that weathering is capable of producing almost pure platinum.

The submicrometric crystals of hongshiite (Figs. 2b, c) do not show any evidence of weathering. The presence of a delicate fabric of hongshiite on octahedral crystals points to open-space precipitation on the reactive surface of a mineral. Inasmuch as magnetite is the oldest (metamorphic) iron oxide phase in the Itabira Iron Formation (Rosière 1981, Pires 1995), showing a distinctive octahedral habit, we believe that the precursor phase was magnetite. No relics of magnetite could be found during the SEM investigation, indicating extensive replacement by hongshiite. It is probable that mag-

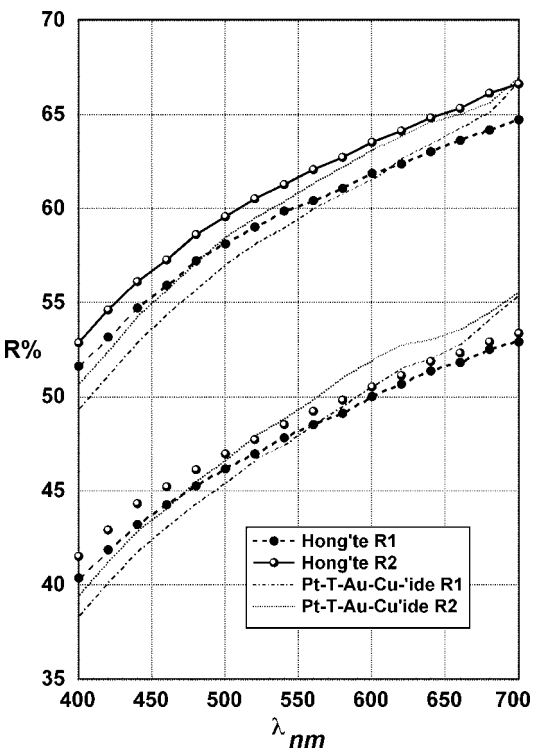

FIG. 7. Reflectance spectra for hongshiite and platinian tetrauricupride.

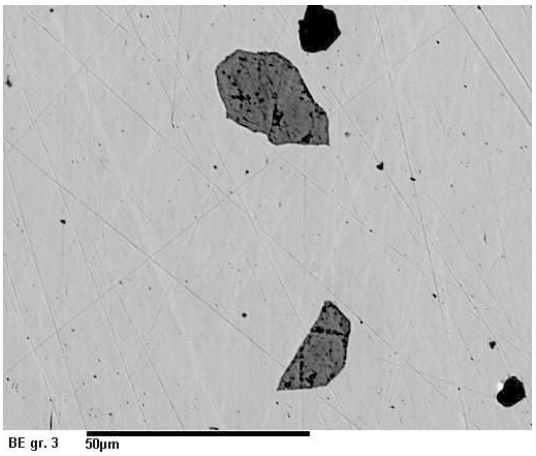

FIG. 8. BSE image of hongshiite containing subhedral inclusions of sudovikovite (dark gray) and an undefined Cu selenide (black).

netite acted not only as a template, but also as a precipitating agent for hongshiite. If so, this event must have occurred before the transformation of magnetite to hematite due to weathering, a widespread phenomenon in the Itabira Iron Formation. Thus, the formation of hongshiite after magnetite seems to be unrelated to supergene processes and may be considerated to be part of the hydrothermal mineralization leading to the jacutinga.

The ubiquitous association of gold and hematite is a characteristic feature of the jacutinga ore, a fact long known (Henwood 1871) and recently emphasized (Olivo *et al.* 1995). The absence of sulfide minerals (Hussak 1906) is evidence for the involvement of oxidized fluids poor in reduced sulfur. Under such conditions, chloride complexing may be responsible for the hydrothermal transport of platinum and copper, and gold and palladium (e.g., Mountain & Wood 1988, Wood & Samson 1998). Reconnaissance study of fluid inclusions in quartz from jacutinga orebodies at Cauê showed one population of aqueous fluid inclusions with tempera-

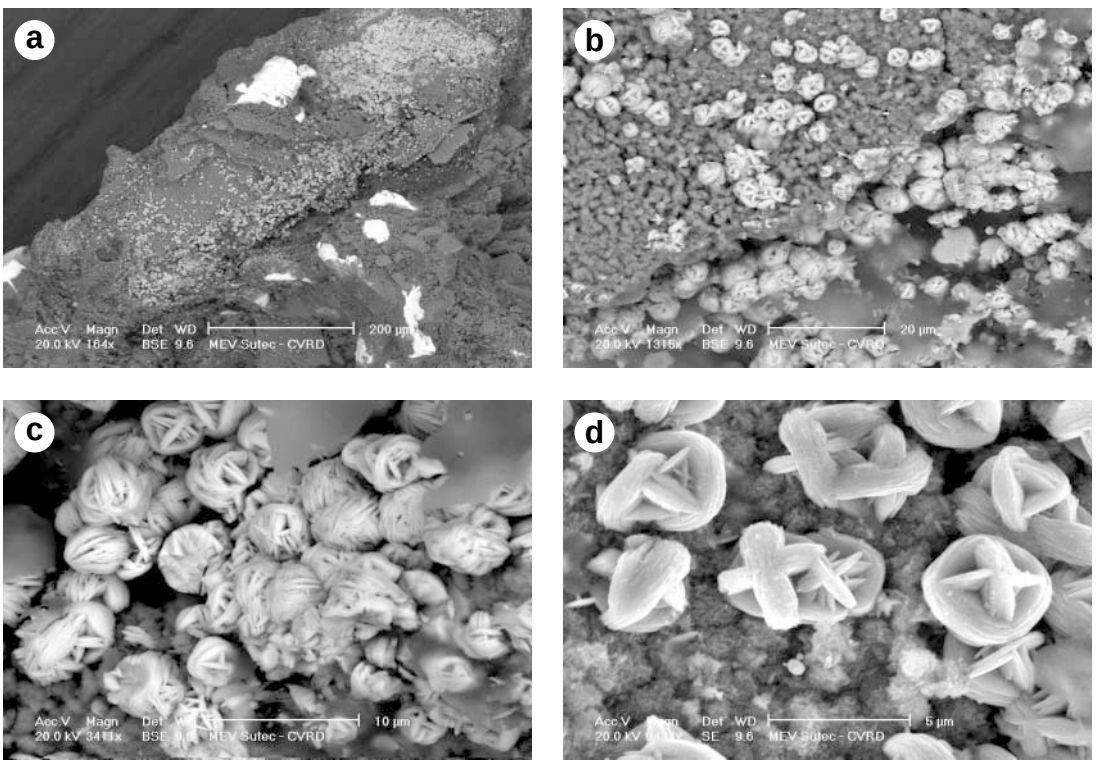

FIG. 9. SEM images of the native palladium rosettes from the Aba Leste Inferior orebody. a. BSE image of iron oxyhydroxide (dark gray) with native gold (white) and scattered fine crystals of native palladium (light gray). b. BSE image with closer view, showing the intimate association of iron oxyhydroxide and rosette-like native palladium on the particle surface. c. BSE image of a cluster of native palladium rosettes. d. SEM image of the orthogonal-disc framework responsible for the rosette pattern of native palladium.

tures of total homogenization and salinities up to 180°C and 15 wt.% NaCl equiv., respectively, indicating involvement of a Cl-bearing aqueous fluid (Galbiatti 1999). Reaction of this fluid with a reducing phase like magnetite would cause effective precipitation of metals (Jaireth 1992). It is therefore possible to consider the hongshiite shown in Figure 2 to be a product of the reducing reaction between an oxidizing Pt- and Cu-bearing fluid and magnetite under temperature conditions compatible with those obtained by microthermometry. Such a redox reaction may be represented by:

$$[PtCl_4]^{2-} + [CuCl_2]^{-} + 2\ Fe_3O_4 + 3/2\ H_2O = PtCu + 3\ Fe_2O_3 + 6\ Cl^{-} + 3\ H^{+} + 1/4\ O_2$$

The existence of tiny euhedral inclusions of barite in hongshiite is noteworthy. Barite precipitates from oxidizing saline fluids over a temperature range up to 300°C (Blount 1977). This is far below the 600°C claimed by Olivo *et al.* (1995) for the jacutinga mineralization.

Acknowledgements

The authors gratefully acknowledge the Companhia Vale do Rio Doce (CVRD) for the support to SEM investigation and permission to publish data. Part of this work benefitted from a Ph.D. scholarship (ARC) by the Deutscher Akademischer Austauschdienst (DAAD). ARC is indebted to Klaus Herrmann (TU Clausthal) for assistance in the electron-microprobe analyses. JHGL and LJC are also grateful to Paul Carrière (CANMET) for the X-ray powder diffraction and to Andy Roberts (GSC) for trying to find a suitable single crystal. We thank Stanislav S. Gornostayev and Gema R. Olivo for their comments, and Robert F. Martin for his careful editing.

References

Alkmim, F.F. & Marshak, S. (1998): Transamazonian orogeny in the southern São Francisco craton region, Minas Gerais, Brazil: evidence for Paleoproterozoic collision and collapse in the Quadrilátero Ferrífero. *Precamb. Res.* **90**, 29-58.

Blount, C.W. (1977): Barite solubilities and thermodynamic quantities up to 300°C and 1400 bars. *Am. Mineral.* **62**, 942-957.

Cabral, A.R., Lehmann, B., Kwitko, R., Jones, R.D., Pires, F.R.M., Rocha Filho, O.G. & Innocentini, M.D. (2001): Palladium-oxygenated compounds of the Gongo Soco mine, Quadrilátero Ferrífero, central Minas Gerais, Brazil. *Mineral. Mag.* **65**, 169-179.

Cabri, L.J. (1980): New mineral names. *Am. Mineral.* **65**, 408.

_____ (1981): Relationship of mineralogy to the recovery of PGE from ores. *In* Platinum-Group Elements: Mineralogy, Geology, Recovery (L.J. Cabri, ed). *Can. Inst. Mining Metall., Spec. Vol.* **23**, 233-250.

_____ & Chao, G.Y. (1978): New mineral names. *Am. Mineral.* **63**, 426.

_____, Clark, A.M. & Chen, T.T. (1977): Arsenopalladinite from Itabira, Brazil, and from the Stillwater complex, Montana. *Can. Mineral.* **15**, 70-73.

_____, Harris, D.C. & Weiser, T.W. (1996): The mineralogy and distribution of platinum group mineral (PGM) placer deposits of the world. *Explor. Mining Geol.* **5**, 73-167.

_____ & Laflamme, J.H.G. (1981): Analyses of minerals containing platinum-group elements. *In* Platinum-Group Elements: Mineralogy, Geology, Recovery (L.J. Cabri, ed). *Can. Inst. Mining Metall., Spec. Vol.* **23**, 151-173.

_____ & _____ (1997): Platinum-group minerals from the Konder massif, Russian Far East. *Mineral. Rec.* **28**, 97-106.

_____, _____, Stewart, J.M., Rowland, J.F. & Chen, T.T. (1975): New data on some palladium arsenides and antimonides. *Can. Mineral.* **13**, 321-335.

Chao, G.Y. & Cabri, L.J. (1976): New mineral names. *Am. Mineral.* **61**, 185.

Chemale, F., Jr. (1987): *Tektonische, lagerstättenkundliche und petrographische Untersuchungen im Eisenerzrevier Itabira, Minas Gerais, Brasilien*. Clausthaler Geowiss. Diss., Technische Universität Clausthal, Clausthal-Zellerfeld, Germany.

_____, Rosière, C.A. & Endo, I. (1994): The tectonic evolution of the Quadrilátero Ferrífero, Minas Gerais, Brazil. *Precamb. Res.* **65**, 25-54.

Clark, A.M., Criddle, A.J. & Fejer, E.E. (1974): Palladium arsenide–antimonides from Itabira, Minas Gerais, Brazil. *Mineral. Mag.* **39**, 528-543.

Colin, F., Sanfo, Z., Brown, E., Bourlès, D. & Minko, A.E. (1997): Gold: a tracer of the dynamics of tropical laterites. *Geology* **25**, 81-84.

Davis, R.J., Clark, A.M. & Criddle, A.J. (1977): Palladseite, a new mineral from Itabira, Minas Gerais, Brazil. *Mineral. Mag.* **41**, 123, M10-13.

Ding, Kuishou (1980): Further studies of the minerals "isoplatinocopper" and hongshiite. *Scientia Geol. Sinica* **2**, 167-171.

Dorr, J.V.N., II (1969): Physiographic, stratigraphic and structural development of the Quadrilátero Ferrífero, Minas Gerais, Brazil. *U.S. Geol. Surv., Prof. Pap.* **641-A**.

_____ & Barbosa, A.L.M. (1963): Geology and ore deposits of the Itabira district, Minas Gerais, Brazil. *U.S. Geol. Surv., Prof. Pap.* **341-C**.

GALBIATTI, H.F. (1999): *Natureza e controle estrutural da mineralização aurífera (jacutinga) na mina do Cauê, Itabira, MG*. M.Sc. thesis, Departamento de Geologia, Universidade Federal de Ouro Preto, Ouro Preto, Brazil.

GUIMARÃES, D. (1970): Arqueogênese do ouro na região central de Minas Gerais. *Departamento Nacional da Produção Mineral, Divisão de Fomento da Produção Mineral (Rio de Janeiro), Boletim* **139**.

HARDER, E.C. & CHAMBERLIN, R.T. (1915): The geology of central Minas Geraes, Brazil. *J. Geol.* **23**, 341-378.

HENWOOD, W.J. (1871): On the gold mines of Minas Geraes, Brazil. *Trans. Royal Geol. Soc. Cornwall* **8**, 168-370.

HIPPERTT, J. & DAVIS, B. (2000): Dome emplacement and formation of kilometre-scale synclines in a granite–greenstone terrain (Quadrilátero Ferrífero, southeastern Brazil). *Precamb. Res.* **102**, 99-121.

HOEFS, J., MÜLLER, G. & SCHUSTER, A.K. (1982): Polymetamorphic relations in iron ores from the Iron Quadrangle, Brazil: the correlation of oxygen isotope variations with deformation history. *Contrib. Mineral. Petrol.* **79**, 241-251.

HUSSAK, E. (1906): O palladio e a platina no Brazil. *Annaes da Escola de Minas de Ouro Preto* **8**, 77-189.

JAIRETH, S. (1992): The calculated solubility of platinum and gold in oxygen-saturated fluids and the genesis of platinum–palladium and gold mineralization in the unconformity-related uranium deposits. *Mineral. Deposita* **27**, 42-54.

JEDWAB, J., CASSEDANNE, J., CRIDDLE, A.J., RY, P. DU, GHYSENS, G., MEISSER, N., PIRET, P. & STANLEY, C.J. (1993): Rediscovery of palladinite PdO from Itabira (Minas Gerais, Brazil) and from Ruwe (Shaba, Zaire). *Terra Nova, Abstract Suppl.* **2**, 22.

KLEIN, C. & LADEIRA, E.A. (2000): Geochemistry and petrology of some Proterozoic banded iron-formations of the Quadrilátero Ferrífero, Minas Gerais, Brazil. *Econ. Geol.* **95**, 405-428.

LOBATO, L.M., RIBEIRO-RODRIGUES, L.C., ZUCCHETTI, M., NOCE, C.M., BALTAZAR, O.F., DA SILVA, L.C. & PINTO, C.P. (2001): Brazil's premier gold province. I. The tectonic, magmatic and structural setting of the Archean Rio das Velhas greenstone belt, Quadrilátero Ferrífero. *Mineral. Deposita* **36**, 228-248.

MCDONALD, I., OHNENSTETTER, D., ROWE, J.P., TREDOUX, M., PATTRICK, R.A.D. & VAUGHAN, D.J. (1999): Platinum precipitation in the Waterberg deposit, Naboomspruit, South Africa. *S. Afr. J. Geol.* **102**, 184-191.

MOUNTAIN, B.W. & WOOD, S.A. (1988): Chemical controls on the solubility, transport, and deposition of platinum and palladium in hydrothermal solutions: a thermodynamic approach. *Econ. Geol.* **83**, 492-510.

NEKRASOV, I.YA., IVANOV, V.V., LENNIKOV, A.M., SAPIN, V.I., SAFRONOV, P.P., OKTYABRSKIY, R.A. & MOLCHANOVA, G.B. (1999): Native alloys of gold, copper, silver, palladium and platinum from the Kondyor alkali-ultrabasic massif. *In* Geodinamica i Metallogeniya. Dalnauka, Vladivostok, Russia (in Russ.).

NIXON, G.T., CABRI, L.J. & LAFLAMME, J.H.G. (1990): Platinum-group-element mineralization in lode and placer deposits associated with the Tulameen Alaskan-type complex, British Columbia. *Can. Mineral.* **28**, 503-535.

OKRUGIN, A.V., ZAYAKINA, N.V., LESKOVA, N.V., LAPUTINA, I.P. & SHCHERBACHEV, D.K. (1999): Phase composition of Pt–Cu–Sb alloys from platinum-bearing placer deposits of western Yakutia. *Zap. Vses. Mineral. Obshchest.* **128**(5), 79-84 (in Russ.).

OLIVO, G.R. & GAMMONS, C.H. (1996): Thermodynamic and textural evidences for at least two stages of Au–Pd mineralization at the Cauê iron mine, Itabira district, Brazil. *Can. Mineral.* **34**, 547-557.

_____ & GAUTHIER, M. (1995): Palladium minerals from the Cauê iron mine, Itabira district, Minas Gerais, Brazil. *Mineral. Mag.* **59**, 455-463.

_____, _____, BARDOUX, M., DE SÁ, E.L., FONSECA, J.T.F. & SANTANA, F.C. (1995): Palladium-bearing gold deposit hosted by Proterozoic Lake Superior-type iron-formation at the Cauê iron mine, Itabira district, southern São Francisco craton, Brazil: geologic and structural controls. *Econ. Geol.* **90**, 118-134.

_____, _____, GARIÉPY, C. & CARIGNAN, J. (1996): Transamazonian tectonism and Au–Pd mineralization at the Cauê mine, Itabira district, Brazil: Pb isotopic evidence. *J. S. Am. Earth Sci.* **9**, 273-279.

_____, _____, WILLIAMS-JONES, A.E. & LEVESQUE, M. (2001): The Au–Pd mineralization at the Conceição iron mine, Itabira district, southern São Francisco craton, Brazil: an example of a jacutinga-type deposit. *Econ. Geol.* **96**, 61-74.

PENG, Z., CHANG, C. & XIMEN, L. (1978): Discussion of published articles in the research of new minerals of the platinum-group discovered in China in recent years. *Acta Geol. Sinica* **4**, 326-336 (in Chinese, with English abstr.).

PIRES, F.R.M. (1995): Textural and mineralogical variations during metamorphism of the Proterozoic Itabira Iron Formation in the Quadrilátero Ferrífero, Minas Gerais, Brazil. *An. Acad. Bras. Ciências* **67**, 77-105.

POLEKHOVSKII, YU.S., TARASOVA I.P., NESTEROV, A.R., PAKHOMOVSKII, YA.A. & BAKHCHARAITSEV, A.YU. (1997): Sudovikovite $PtSe_2$ – a new platinum selenide from south Karelia metasomatites. *Dokl. Akad. Nauk* **354**, 486-489.

ROSIÈRE, C.A. (1981): *Strukturelle und texturelle Untersuchungen in der Eisenerzlagerstätte "Pico de Itabira" bei Itabirito, Minas Gerais, Brasilien*. Clausthaler Geowiss. Diss., Technische Universität Clausthal, Clausthal–Zellerfeld, Germany.

SWEENY, J.M. (1989): *The Geochemistry and Origin of Platinum Group Element Mineralization of the Hybrid Zone, Lac des Iles Complex, Northwestern Ontario*. M.Sc. thesis, Univ. of Western Ontario, London, Canada.

TOLSTYKH, N.D., KRIVENKO, A.P. & BATURIN, S.G. (1996): Compositional features of native platinum from different mineral assemblages of platinum-group elements. *Geologiya i Geofizica* **37**, 39-46 (in Russ.).

_____, _____ & POSPELOVA, L. (1997): New compounds of Ir, Os and Ru with selenium, arsenic and tellurium. *Eur. J. Mineral.* **9**, 457-465.

_____, SIDOROV, E.G., LAAJOKI, K.V.O., KRIVENKO, A.P. & PODLIPSKIY, M. (2000): The association of platinum-group minerals in placers of the Pustaya River, Kamchatka, Russia. *Can. Mineral.* **38**, 1251-1264.

TÖRNROOS, R. & VUORELAINEN, Y. (1987): Platinum-group metals and their alloys in nuggets from alluvial deposits in Finnish Lapland. *Lithos* **20**, 491-500.

VARAJÃO, C.A.C., COLIN, F., VIEILLARD, P., MELFI, A.J. & NAHON, D. (2000): Early weathering of palladium gold under lateritic conditions, Maquiné mine, Minas Gerais, Brazil. *Appl. Geochem.* **15**, 245-263.

WEISER, T. & SCHMIDT-THOMÉ, M. (1993): Platinum-group minerals from the Santiago River, Esmeraldas Province, Ecuador. *Can. Mineral.* **31**, 61-73.

WOOD, S.A. & SAMSON, I.M. (1998): Solubility of ore minerals and complexation of ore metals in hydrothermal solutions. *Rev. Econ. Geol.* **10**, 33-80.

YU, ZUXIANG (1982): New data on hongshiite. *Bull. Inst. Geol., Chinese Acad. Geol. Sci.* **4**, 78-81 (in Chinese, with English abstr.).

_____ (1986): Some new minerals from platinum-bearing rocks in Yanshan and Tibet regions, China. *Bull. Inst. Geol., Chinese Acad. Geol. Sci.* **15**, 49-57 (in Chinese, with English abstr.).

_____ (2001): New data for hongshiite. *Acta Geol. Sinica* **75**, 400-403 [in Chinese, with Engl. abstr.; see *Mineral. Abstr*. **53**(1), O2M/0809, p. 98].

_____*, LIN, SHU-JEN, CHAO, PAO, FANG, CHING-SUNG, & HUANG, CHI-SUNG (1974): A preliminary study of some new minerals of the platinum group and another associated new one in platinum-bearing intrusions in a region in China. *Acta Geol. Sinica* **2**, 202-218 (in Chinese, with English abstr.) (* formerly transliterated Yu, Tsu-Hsiang).

Received September 18, 2001, revised manuscript accepted February 2, 2002.